Journal of Colloid and Interface Science 329 (2009) 410–415

Contents lists available at ScienceDirect

Journal of Colloid and Interface Science

www.elsevier.com/locate/jcis

Hybrid QM/MM simulation of the hydration phenomena of dipalmitoylphosphatidylcholine headgroup

Jun Yin, Ya-Pu Zhao *

State Key Laboratory of Nonlinear Mechanics (LNM), Institute of Mechanics, Chinese Academy of Sciences, Beijing 100190, China

ARTICLE INFO

Article history:
Received 7 August 2008
Accepted 19 September 2008
Available online 1 October 2008

Keywords:
Hydration
Hybrid QM/MM simulation
ONIOM
DPPC
Polar headgroup
Hydrogen bond

ABSTRACT

The polar headgroup of dipalmitoylphosphatidylcholine (DPPC) molecule both in gas phase and aqueous solution is investigated by the hybrid quantum mechanical/molecular mechanical (QM/MM) method, in which the polar head of DPPC molecule and the bound water molecules are treated with density functional theory (DFT), while the apolar hydrocarbon chain of DPPC molecule is treated with MM method. It is demonstrated that the hybrid QM/MM method is both accurate and efficient to describe the conformations of DPPC headgroup. Folded structures of headgroup are found in gas phase calculations. In this work, both monohydration and polyhydration phenomena are investigated. In monohydration, different water association sites are studied. Both the hydration energy and the quantum properties of DPPC and water molecules are calculated at the DFT level of theory after geometry optimization. The binding force of monohydration is estimated by using the scan method. In polyhydration, more extended conformations are found and hydration energies in different polyhydration styles are estimated.

1. Introduction

The physical and chemical properties of biological membranes are of critical importance for understanding specific membrane functions, such as material transport across membranes and communication between cells. The predominant interest in phospholipid bilayers arises because they are one of the major, if not the major, structural elements of biological membranes [1]. Some properties of biological membranes can be directly attributed to the characteristics of single phospholipid molecules. Due to their important role, phospholipids are the subject of numerous experimental and computational studies in recent decades [2–8].

As an amphiphile, the two principal features of a typical phospholipid molecule are hydrophilic polar headgroup and hydrophobic hydrocarbon chain. In many previous works [3,5,9–13], a detailed structural knowledge of the biological membrane is particularly associated with the conformation and interactions of polar phospholipid headgroups at the membrane surface. In many previous quantum mechanical researches, it is shown that the polar headgroups of the phospholipids manifest an intrinsic preference towards folded structures stabilized by strong intramolecular hydrogen bonds (Fig. 1) or electrostatic interaction between the phosphate group and the cationic head in gas phase [3,5,9]. X-ray experimental studies [14] also indicate that the polar headgroups of phospholipids tend to favor certain conformations. But further calculations suggest that if hydration [10] or the presence of neighboring headgroups is taken into account, the polar headgroups of phospholipids adopt the more extended form in crystals. Their existence in the extended form in the crystals and possibly in water must be attributed to the effect of the intermolecular forces [15].

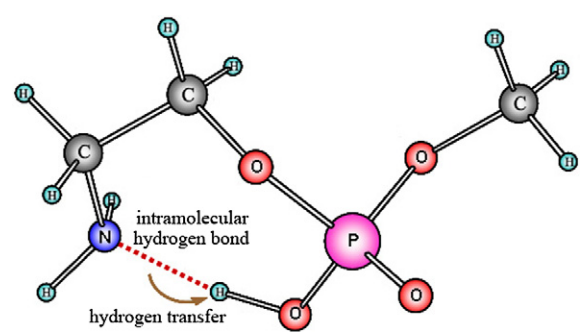

Fig. 1. The preferred conformation of the headgroup of phospholipids in gas phase.

The most obvious property of phospholipid headgroup is its strong polar dipole. As we know, hydrated water molecules bind to polar dipoles by forming hydrogen bonds, so phospholipid molecules are inclined to act in the aqueous solution in hydrated form [16]. A hydrogen bond results when strong positive charge density of a hydrogen atom attracts a lone pair of electrons on another heteroatom. Some parts of polar groups of phospholipid molecules, such as phosphate, carboxyl, and carbonyl are most

* Corresponding author. Fax: +86 10 6256 1284.
E-mail address: yzhao@imech.ac.cn (Y.-P. Zhao).

0021-9797/$ – see front matter
doi:10.1016/j.jcis.2008.09.070

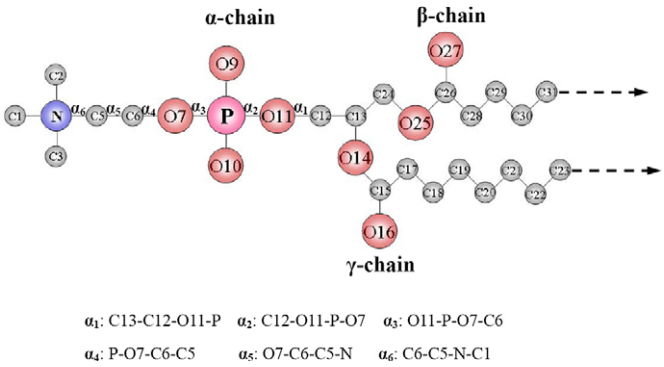

Fig. 2. Atom labeling and notation for the dihedral angles for DPPC ($C_{40}H_{80}NO_8P$) molecule. All the hydrogen atoms are omitted in this figure, but are included in all calculations.

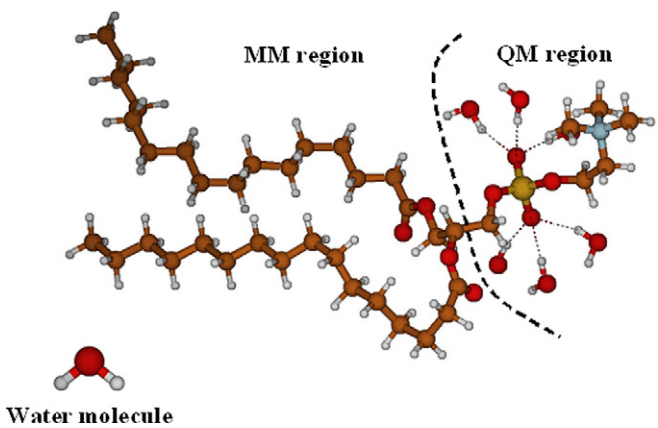

Fig. 3. The partition of DPPC and hydrated water molecules into QM and MM regions.

strongly affected by hydrated water molecules, therefore phospholipid hydrophilicity depends on the participation of these groups in forming hydrogen bonds. The phospholipid molecule and its hydrated water act as a single thermodynamic and physicochemical entity [1]. The complex phase behavior of phospholipid–water systems is in relation to many biological functions of biological membranes, so the interaction between polar headgroup and water is of special interest. Hydration of the hydrocarbon chain is much weaker and restricted to the interactions at the polar–apolar interface; therefore this study mainly focuses on the headgroup region of phospholipid molecules.

The most prevalent phospholipid molecule that forms the bilayer of eukaryotic cell membranes is phosphatidylcholine (PC). DPPC (Fig. 2) is an amphiphilic molecule with a polar headgroup (α-chain) and two hydrophobic hydrocarbon chains (β- and γ-chains) [17]. DPPC is a kind of saturated PC which is studied adequately both by experiment and calculation [2,4,6,7,18], so DPPC is used as a typical example of phospholipid molecules for calculations in this work.

In order to study the hydration phenomena of DPPC headgroup, the hybrid QM/MM method is applied in this work. Although there are numerous previous computational studies [3,5,9–13], which analyzed the structure and hydration of phospholipid headgroup. Considering the limits of computing ability, the majority of these investigations have used short chain molecules (e.g. just headgroup) rather than the whole phospholipid molecules to study the headgroup region of phospholipid molecules. But the structure of the isolated polar head group could be different from that of the same group in the entire molecule. In order to make a suitable compromise between the quality of simulation results and the requirement of CPU time, the hybrid QM/MM method is performed

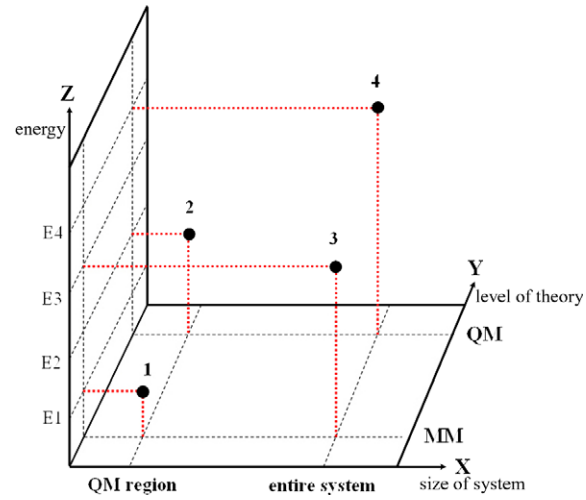

Fig. 4. The diagrammatic presentation of ONIOM method for a partitioned molecular system.

on a whole DPPC molecule in this work. In the hybrid QM/MM technique, the chemically most relevant region is treated by Born–Oppenheimer ab initio quantum mechanics, while the rest of the system is described by MM potentials [19,20]. The DPPC hydration phenomena are very suitable for using the hybrid QM/MM method, because it is demonstrated that the properties of the headgroup of phospholipid are affected by the hydrocarbon chain slightly, no matter the degree of N-methylation [3,12]. In geometry optimization, the headgroup and its bound water molecules are treated at QM level of theory and the hydrocarbon chain with MM method (Fig. 3).

In this work, first the hybrid QM/MM method is demonstrated to be both accurate and efficient enough to describe the conformations of DPPC headgroup. Then, both monohydration and polyhydration phenomena are investigated.

2. Numerical method

In this work, all QM/MM and pure QM calculations are done with the Gaussian03 [21] ab initio packages. For QM/MM calculations, the ONIOM ("our own n-layered integrated molecular orbital and molecular mechanics") [22] implementation in Gaussian03 is used. The coupling between the QM and MM regions in ONIOM approach is embodied in ONIOM energy definition. A QM/MM system energy definition in ONIOM approach is shown in Fig. 4, where the X axis is the size of the system, the Y axis is the level of theory, and the Z axis is the energy. The ONIOM energy of the entire system E_{ONIOM} is defined as:

$$E_{\mathrm{ONIOM}} = E_3 - E_1 + E_2, \tag{1}$$

where E_3 is the entire system energy calculated at the MM level, while E_1 and E_2 are energies of QM region calculated at the MM and QM level, respectively. E_{ONIOM} is an approximation to the QM level energy of the entire system E_4,

$$E_4 = E_{\mathrm{ONIOM}} + D. \tag{2}$$

It is assumed that the error D of the extrapolation procedure is constant for each structure. So the relative energy different $\Delta E_4 = E_4^A - E_4^B$ for two different conformations A and B (e.g. hydrated and non-hydrated structures) will be evaluated approximately by the ONIOM energy $\Delta E_{\mathrm{ONIOM}} = E_{\mathrm{ONIOM}}^A - E_{\mathrm{ONIOM}}^B$ [23]. The validity of ONIOM approach for accurate calculation has been affirmed [22–24], already.

All the geometry optimizations are carried out using the hybrid QM/MM method without any constrains, and hydrogen atoms

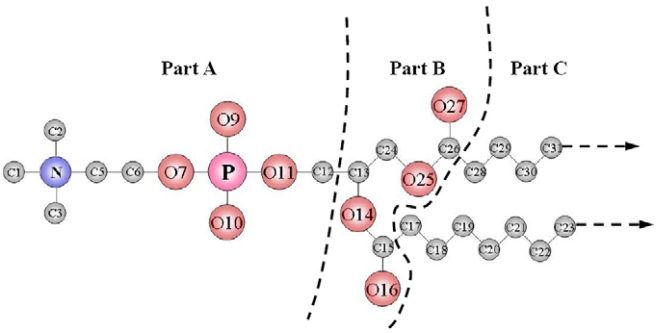

Fig. 5. The partition DPPC molecule into three parts for illustration of four computational models.

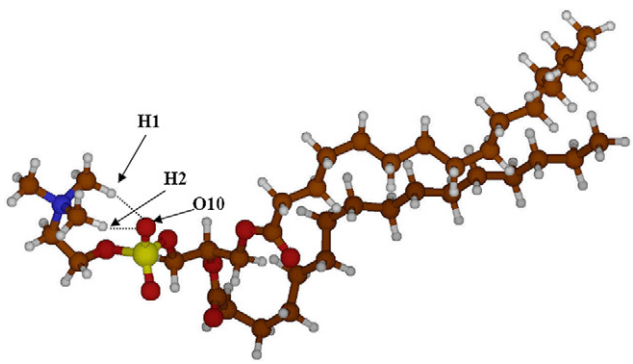

Fig. 6. The optimized conformation of DPPC molecule in gas phase by the hybrid QM/MM method. Dashed lines represent hydrogen bonds.

are used as link atoms. QM region is treated with DFT, while in MM region, UFF (a universal force field) [25] is used. In DFT calculations, we employ Becke's non-local three-parameter exchange and correlation functional [26] with the Lee–Yang–Parr correlation functional [27]. The hybrid functional, B3LYP is demonstrated to give results with an accuracy similar to that of an MP2 (second-order perturbation) calculation in bonding energy and geometry optimization for hydrogen-bonded systems [28,29]. 6-31++G(d) basis set is used in DFT calculations, because both diffuse functions and d-type polarization functions for all heavy atoms does provide the best description of phospholipid headgroups [3], and in hydration phenomena hydrogen bonds can only be correctly described by including diffuse functions into basis sets. In MM region, the potential energy of an arbitrary geometry in UFF is written as a superposition of various two-body, three-body, and four-body interactions. The parameters of UFF are described in Rappe et al.'s paper (1992) in detail [25]. Single point calculations on QM/MM optimized geometries by the pure QM method are carried out at B3LYP/6-31++G(d) level of theory. In a word, B3LYP/6-31++G(d)//(B3LYP/6-31++G(d):UFF) is used in calculations.

In order to evaluate the binding force of monohydration water molecule to DPPC headgroup, we perform relaxed potential energy surface (PES) scan (with geometry optimization at each point) where hydrogen bonds of hydrated water molecules are stretched by 0.05 nm per step. Because of computational cost, the relaxed PES scans are performed in the QM/MM level (B3LYP/6-31++G(d):UFF), which is the same as geometry optimizations.

3. Results and discussions

3.1. DPPC headgroup in gas phase

In order to demonstrate the accuracy of the hybrid QM/MM method used in this work to describe crucial region of headgroup, four models of QM/MM calculations with different partition of QM/MM regions are performed. In Fig. 5, a DPPC molecule is divided into three parts. In model I, the QM region is part A, and the MM region consists of part B and part C. In model II, the QM region includes part A and part B, and part C is the MM region. In model III, two more atoms than model II (C17 and C28) is added into the QM region, and in model IV another two atoms (C18 and C29) are added to the QM region than model III. From model I to model IV more atoms are put into QM region and it is more time consuming. In Table 1, there are some chief optimized geometrical parameters of four models. It is found that though the QM region becomes lager, the optimized geometry of the DPPC headgroup dose not vary drastically. The biggest difference of O–P bond length is about 0.01 Å (bond P–O7 between model I and II). As a crucial parameter in DPPC headgroup, P---N distance also differs slightly, only 0.03 Å (between model I and IV). For angles, the biggest difference is 0.18° in O7–P–O11 between model I and III. The most fluctuating parameter is dihedral angle and 8.58° is the biggest difference (in α_3 between model I and IV). From these results, it can be concluded that the headgroup is slightly affected by the hydrocarbon chain region, so the hybrid QM/MM method used in this work is very suitable to describe the conformation of headgroup of DPPC molecule. Consideration of computational cost and accuracy, model I is employed to divide the QM and MM regions of DPPC molecule in all following calculations.

Table 1
Structural parameters of different QM/MM models.

		Model I	Model II	Model III	Model IV
Bond length (Å)	P–O7	1.7192	1.7078	1.7098	1.7137
	P–O9	1.4979	1.5001	1.4993	1.4977
	P–O10	1.5139	1.5106	1.5118	1.5118
	P–O11	1.6266	1.6350	1.6331	1.6346
Non-bond length (Å)	P---N	4.0016	3.9901	3.9976	3.9725
Angle	O9–P–O10	123.09	122.96	123.00	122.96
	O7–P–O11	96.95	97.02	97.13	97.05
Dihedral angle	α_1	−151.17	−149.39	−150.33	−153.71
	α_2	−78.61	−74.80	−76.50	−76.56
	α_3	175.30	171.09	173.68	166.72
	α_4	123.53	122.42	123.09	121.29
	α_5	−66.24	−66.19	−66.30	−65.26
	α_6	−169.57	−168.17	−168.93	−167.19

Dihedral angle is in the range of −180° to 180°.

The optimized structure of DPPC in gas phase by the hybrid QM/MM method is displayed in Fig. 6. It should be noticed that the optimized cyclic conformation is stabilized by electrostatic attractions between hydrogen atoms (especially H1 and H2 in Fig. 6) of the choline methyl groups and the phosphate oxygen atoms (especially O10 in Fig. 6), giving rise to H---O distance (H1---O10 is 2.046 Å and H2---O10 is 2.051 Å) that are considerably shorter than normal van der Waals radii (2.72 Å) of hydrogen atom (1.2 Å) plus oxygen atom (1.52 Å). In the case of DPPC, the cationic part is much bulker due to the three *N*-methyl groups, and the three methyl groups extend the P---N distance (in this work is 4.001 Å, which is 3.94 Å in Li and Lagowski's paper, 1999). So there just forms two hydrogen bonds, and the H^+-transfer reaction (shown in Fig. 1) is not favorable, but the electric charge transfer phenomenon is still very obvious. In Table 3 (the first column), the electropositivity value of H1 and H2 is larger than other hydrogen atoms in choline methyl groups (other hydrogen atoms are less than 0.3) and O10 is more electronegative than other phosphate oxygen atoms. Therefore, it is electrostatic attraction that makes the DPPC this folded structure in gas phase.

3.2. Monohydration

One water molecule and a DPPC molecule (model I) are taken into account for monohydration. It has been proved that in the DPPC polar head, there are obviously two principal hydration regions: the cationic $N^+(CH_3)_3$ end and the oxygen atoms in phosphate group [12]. If only oxygen atoms association is considered, there are two forms: one is one of water O–H bonds directed to a oxygen atom while leaving the second water O–H bond free in space (all of four oxygen atoms are calculated respectively), the other is in a bridge position with respect to the two ester oxygen atoms (O9 and O10) involved (Fig. 7).

The hydration energy is calculated by Eq. (3)

$$\Delta E_{\text{hydration}} = -\frac{1}{n}\left[E\left(\text{DPPC}\cdot(\text{H}_2\text{O})_n\right) - E(\text{DPPC}) - E\left((\text{H}_2\text{O})_n\right)\right], \quad (3)$$

where $n = 1$ in monohydration. In Table 2, the hydration energy of $N^+(CH_3)_3$ group is obviously lower than that of oxygen atoms in phosphate group. The hydrogen bond length between hydrogen atom in $N^+(CH_3)_3$ group and oxygen atom in hydrated water molecule is longer other hydrogen bonds in DPPC monohydration, which shows that it is a weak hydrogen bond. The hydration energy of $N^+(CH_3)_3$ group is lower than hydration energy between two water molecules (about 28 KJ/mol).

Tables 2 and 3 show that hydration effect is intense on oxygen atoms in phosphate group, especially on two ester atoms (O9 and O10). There are some traits: (a) the binding energy of these monohydration is much higher than hydration energy between two water molecules (about 28 KJ/mol). These hydrogen bonds are more stable, so water molecules prefer to hydrate with oxygen atoms in DPPC headgroup rather than with other water molecules; (b) the bond length of these hydrogen bonds is much shorter than normal van der Waals radii (2.72 Å) of hydrogen and oxygen atoms. The bond length of O–H* (H* is the hydrogen atom of water molecule which forms the hydrogen bond with DPPC) in hydrated water molecules is longer than the other O–H bond length in water molecule, because of attraction between H* atom and oxygen atom of DPPC molecule; (c) charge transfer is noticeable. Oxygen atoms are more electropositive when they are hydrated, while H* atom

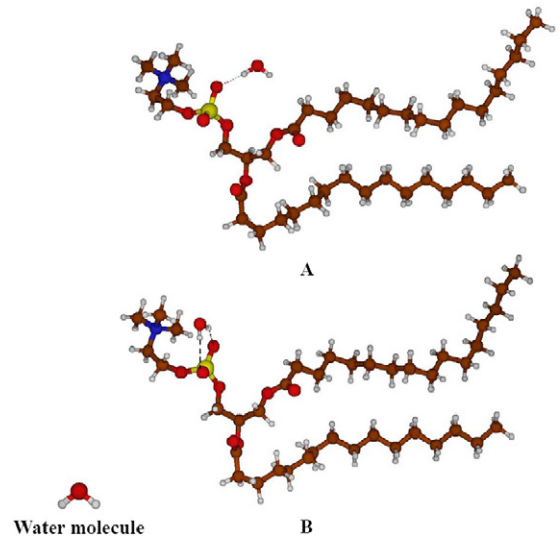

Fig. 7. Two forms of monohydration: A is one of water O–H bonds directed to a oxygen atom while leaving the second water O–H bond free in space; B is water molecule in a bridge position with respect to the two ester oxygen atoms (O9 and O10) involved. Dashed lines represent hydrogen bonds.

Table 2
Structural parameters, hydration energy, bonding force and Mulliken population analysis of monohydrated water molecule (for hydration on bridge position and hydration with $N^+(CH_3)_3$, H* and H are the same).

		Hydration with O7	Hydration with O9	Hydration with O10	Hydration with O11	Hydration on bridge	Hydration with $N^+(CH_3)_3$
Mulliken population analysis of water molecule	H*	0.66	0.64	0.65	0.54	0.60	0.49
	H	0.50	0.50	0.48	0.49	0.53	0.48
	O	−1.07	−1.07	−1.06	−1.00	−1.00	−0.97
Water molecule Bond length (Å)	O–H*	0.9842	0.9950	0.9874	0.9820	0.9846	0.9704
	O–H	0.9680	0.9677	0.9677	0.9687	0.9753	0.9702
Hydrogen bond length (Å)	O---H	1.8500	1.7461	1.7683	1.8622	1.9053 2.1990	2.4190
Hydration energy (KJ/mol)		48.57	66.69	59.86	45.16	71.15	22.84
Bonding force (pN)		322.6	505.7	645.3	357.5	–	–

In Mulliken population analysis, charges are in electron units.

Table 3
Summary of Mulliken population analysis (obtained with B3LYP/6-31++G(d)) for DPPC molecule in gas phase and monohydration respectively.

	Gas phase	Hydration with O7	Hydration with O9	Hydration with O10	Hydration with O11	Hydration on bridge	Hydration with $N^+(CH_3)_3$
C1	−0.29	−0.28	−0.32	−0.28	−0.30	−0.25	−0.30
C2	−0.43	−0.44	−0.41	−0.45	−0.35	−0.38	−0.40
C3	−0.43	−0.44	−0.48	−0.41	−0.43	−0.32	−0.46
N	−0.74	−0.76	−0.72	−0.76	−0.75	−0.82	−0.70
C5	−0.05	−0.02	−0.08	−0.06	−0.05	−0.06	−0.04
C6	−0.46	−0.51	−0.48	−0.45	−0.40	−0.42	−0.50
O7	−0.64	−0.77	−0.65	−0.64	−0.62	−0.63	−0.64
P	1.93	1.96	1.85	2.08	1.97	1.90	2.12
O9	−0.76	−0.74	−0.92	−0.74	−0.73	−0.86	−0.76
O10	−0.84	−0.87	−0.87	−1.14	−0.83	−0.98	−0.86
O11	−0.57	−0.51	−0.53	−0.57	−0.76	−0.53	−0.62
C12	0.14	−0.01	−0.16	0.12	0.17	0.03	0.16
H1	0.32	0.33	0.32	0.34	0.33	0.37	0.26
H2	0.35	0.35	0.38	0.32	0.36	0.21	0.37

In Mulliken population analysis, charges are in electron units.

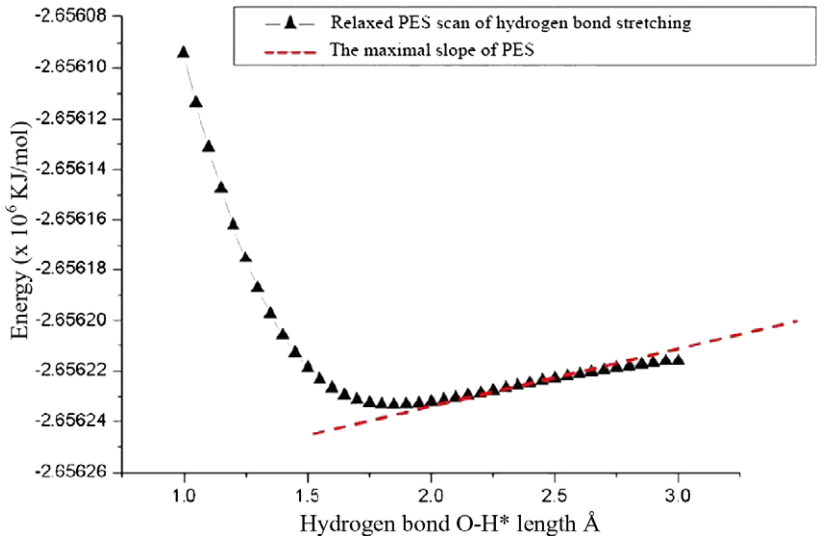

Fig. 8. An example of energy surface of relaxed PES scan of hydrogen bond stretching. Red line indicates the binding force between DPPC headgroup and monohydrated water molecule. (For interpretation of the references to color in this figure legend, the reader is referred to the web version of this article.)

is more electronegative than the other H atom in hydrated water molecule. All of these traits indicate that it forms a strong hydrogen bond between water molecule and oxygen atoms in phosphate group, so on oxygen atoms of phosphate group, the hydration effect is obvious. For hydration in a bridge position, the hydration energy is much higher because two hydrogen bonds are formed, though these two hydrogen bonds are a bit longer and binding energy of each hydrogen bond is lower.

In order to estimate the binding force of these hydrogen bonds, the relaxed PES scan is performed to get the energy surfaces with the hydrogen bond length as x-axis in coordinate (Fig. 8). Hydrogen bonds are stretched from 1 to 3 Å by 0.05 Å per step. The binding force is calculated according to

$$F_{\text{H bond}} = \max\left(\left|-\frac{\partial E}{\partial x}\right|\right). \tag{4}$$

The binding forces of hydrogen bonds with oxygen atoms on DPPC molecule are calculated (e.g. configuration in Fig. 7A), since oxygen atoms are most important hydration sites on DPPC molecule. From Table 2, it is found that the binding forces are in the same order as hydrogen bond rupture force detected by other experiments (10^2 pN). Because relaxed PES scan method carries out geometry optimization at each point, the scan process simulates the rupture of hydrogen bond in a static state. For two ester oxygen atoms (O9 and O10), their hydration energy and binding force are higher than other two oxygen atoms (O7 and O11). Because ester oxygen atom has three lone pair electrons, it is a sensitive hydration site, water molecules are inclined to hydrate with this site.

3.3. Polyhydration

Some experiments have found that in DPPC bilayer, a single DPPC molecule binds about six molecules of water on average [18]. In monohydration, it is clear that the hydration ability of oxygen atoms in phosphate group is stronger than $N^+(CH_3)_3$ group, so it is assumed that hydrated water molecules are mainly bound to oxygen atoms. Theoretically, two ester oxygen atoms (O9 and O10) have three lone pair electrons, so they can bind three water molecules each. Other two oxygen atoms (O7 and O11) have two lone pair electrons; therefore they can bind two water molecules each. The polarity of oxygen atoms will be weakened when they bind one water molecule; and because of the interactions between water molecules and neighboring DPPC molecules, less than ten water molecules can be bound. In our computations, first, three water molecules are bound to two ester oxygen atoms (O9 and O10) respectively. Then six water molecules are bound to the two oxygen atoms (O9 and O10) at the same time. At last, ten water molecules are put around the four oxygen atoms (Fig. 9).

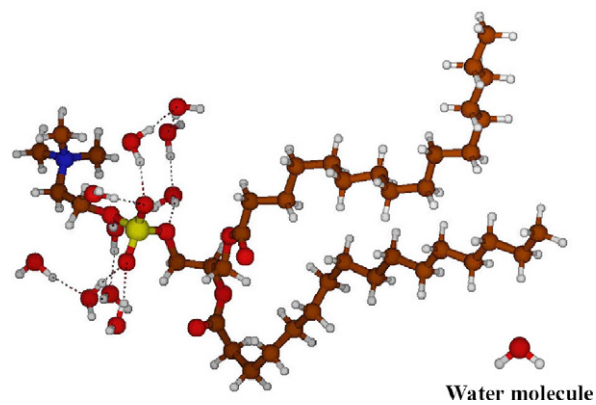

Fig. 9. Polyhydration of DPPC headgroup with ten water molecules. Dashed lines represent hydrogen bonds.

In Table 4, it can be noticed that the hydration energy per water molecule of polyhydration is a little lower than that of monohydration. Because of steric hindrance and electrostatic repulsion between water molecules, water molecules cannot bind to oxygen atoms as tightly as monohydration. When there are ten water molecules, not all the water molecules bind to oxygen atoms of DPPC headgroup directly. There are six water molecules in the first water shell (O9 and O10 bind two water molecules respectively, while O7 and O11 bind one water molecule respectively). Other four water molecules are on the second water shell and interacting mainly with first water shell (Fig. 9). The interaction between water molecules is weaker than that between oxygen atoms of DPPC headgroup and water, so hydration energy of average water molecule is much lower than that of monohydration. The charge transfer is more obvious in polyhydration than monohydration. Both two ester oxygen atoms (O9 and O10) are more electronegative when polyhydrated. Dihedral angles are drastically undulated in different polyhydration conditions, especially is α_1–α_5; while α_6 vary slightly, even their values do not change a lot from gas phase in Table 1. It indicates that ammonium group of DPPC headgroup is less affected by polyhydration. Another noticeable phenomenon in

Table 4
Parameters of polyhydration.

		O9 binds three water molecules	O10 binds three water molecules	O9 and O10 binds six water molecules	Ten water molecules hydration
Hydration energy of average water molecule (KJ/mol)		45.33	58.62	53.71	37.81
Average hydrogen bond length (Å)		2.0346	1.8802	1.9233	–
H1---O10 length (Å)		2.0359	3.1743	3.4903	3.7761
H2---O10 length (Å)		2.3124	2.3257	3.2857	4.1128
Mulliken population analysis	O9	−1.15	−0.74	−1.13	−1.15
	O10	−0.91	−1.30	−1.18	−1.02
N---P distance (Å)		4.0143	4.2706	4.5402	4.7567
Dipole moment of DPPC molecule (Debye)		15.24	18.85	21.49	22.48
Dihedral angle	α_1	−118.80	−159.80	153.23	−128.80
	α_2	−101.74	−76.48	−74.47	−107.27
	α_3	162.48	173.29	171.85	−172.12
	α_4	119.62	146.73	166.87	−179.08
	α_5	−70.00	−62.04	−68.13	−78.81
	α_6	−163.08	−163.16	−167.53	−179.87

In Mulliken population analysis, charges are in electron units. Dihedral angle is in the range of −180° to 180°.

polyhydration is the variation of P---N distance. In these calculations, P---N distance becomes longer when more water molecules are hydrated. Not only polar effect of water, but also steric hindrance makes DPPC headgroup extended. Of course, dipole moments of DPPC molecules increase when DPPC headgroup extends. No intramolecule hydrogen bonds form when O10 is polyhydrated.

4. Summary

This work is focused on hydration phenomena of DPPC headgroup. Because its hydrocarbon chain affects DPPC hydration slightly, the hybrid QM/MM method is used, where DPPC polar headgroup and water molecules are put into QM region.

The QM region is extended to four different models for computations. It is demonstrated that the QM/MM division in this work is accurate enough to investigate the conformation of DPPC polar headgroup. In gas phase, intramolecule hydrogen bonds are found in DPPC headgroup. In monohydration simulation, it is shown that ester oxygen atoms of phosphate group have stronger hydration effect than other groups in DPPC headgroup, and hydration energy exceeds binding energy between water molecules obviously. Through relaxed PES scan method, it can be estimated that the hydration force of oxygen atoms in phosphate group is in the order of 10^2 pN. In polyhydration simulation, hydration energy per water molecule is a little lower than monohydration energy. Extended headgroup structures are found when DPPC is polyhydrated and intramolecule hydrogen bonds are ruptured. The charge transfer phenomenon is noticed in all hydration calculations.

Acknowledgments

This work was jointly supported by the National Basic Research Program of China (973 Program, Grant No. 2007CB310500), the National High-tech R&D Program of China (863 Program, Grant Nos. 2007AA04Z348 and 2007AA021803) and National Natural Science Foundation of China (NSFC, Grant No. 10772180).

References

[1] G. Cevc, D. Marsh, Phospholipid Bilayers, Wiley, New York, 1987.
[2] O. Berger, O. Edholm, F. Jahnig, Biophys. J. 72 (1997) 2002–2013.
[3] J. Landin, I. Pascher, D. Cremer, J. Phys. Chem. 99 (1995) 4471–4485.
[4] Z.V. Leonenko, E. Finot, H. Ma, T.E.S. Dahms, D.T. Cramb, Biophys. J. 86 (2004) 3783–3793.
[5] W. Li, J.B. Lagowski, Chem. Phys. Lipids 103 (1999) 137–160.
[6] S.J. Marrink, O. Berger, P. Tieleman, F. Jahnig, Biophys. J. 74 (1998) 931–943.
[7] H.W. Meyer, K. Semmler, W. Rettig, W. Pohle, A.S. Ulrich, S. Grage, C. Selle, P.J. Quinn, Chem. Phys. Lipids 105 (2000) 149–166.
[8] S.Y. Bhide, M.L. Berkowitz, J. Chem. Phys. 125 (2006) 094713.
[9] B. Pullman, H. Berthod, FEBS Lett. 44 (1974) 266–269.
[10] B. Pullman, H. Berthod, N. Gresh, FEBS Lett. 53 (1975) 199–204.
[11] C.X. Liang, C.S. Ewig, T.R. Stouch, A.T. Hagler, J. Am. Chem. Soc. 115 (1993) 1537–1545.
[12] J. Landin, I. Pascher, D. Cremer, J. Phys. Chem. A 101 (1997) 2996–3004.
[13] K. Kubica, Comput. Chem. 26 (2002) 351–356.
[14] I. Pascher, M. Lundmark, P.G. Nyholm, S. Sundell, Biochim. Biophys. Acta 1113 (1992) 339–373.
[15] R. Brasseur, J.-M. Ruysschaert, Biochem. J. 238 (1986) 1–11.
[16] I.R. Miller, D. Bach, E.J. Wachtel, M. Eisenstein, Bioelectrochemistry 58 (2002) 193–196.
[17] D. Marsh, CRC Handbook of Lipid Bilayers, CRC Press, Boca Raton, 1990.
[18] D. Bach, I.R. Miller, Chem. Phys. Lipids 136 (2005) 67–72.
[19] A. Tongraar, B.M. Rode, Chem. Phys. Lett. 403 (2005) 314–319.
[20] Z.Y. Yang, Y.P. Zhao, Mater. Sci. Eng. A 423 (2006) 84–91.
[21] M.J. Frisch, G.W. Trucks, H.B. Schlegel, G.E. Scuseria, M.A. Robb, J.R. Cheeseman, J.A. Montgomery, T.V. Jr., K.N. Kudin, J.C. Burant, J.M. Millam, S.S. Iyengar, J. Tomasi, V. Barone, B. Mennucci, M. Cossi, G. Scalmani, N. Rega, G.A. Petersson, H. Nakatsuji, M. Hada, M. Ehara, K. Toyota, R. Fukuda, J. Hasegawa, M. Ishida, T. Nakajima, Y. Honda, O. Kitao, H. Nakai, M. Klene, X. Li, J.E. Knox, H.P. Hratchian, J.B. Cross, V. Bakken, C. Adamo, J. Jaramillo, R. Gomperts, R.E. Stratmann, O. Yazyev, A.J. Austin, R. Cammi, C. Pomelli, J.W. Ochterski, P.Y. Ayala, K. Morokuma, G.A. Voth, P. Salvador, J.J. Dannenberg, V.G. Zakrzewski, S. Dapprich, A.D. Daniels, M.C. Strain, O. Farkas, D.K. Malick, A.D. Rabuck, K. Raghavachari, J.B. Foresman, J.V. Ortiz, Q. Cui, A.G. Baboul, S. Clifford, J. Cioslowski, B.B. Stefanov, G. Liu, A. Liashenko, P. Piskorz, I. Komaromi, R.L. Martin, D.J. Fox, T. Keith, M.A. Al-Laham, C.Y. Peng, A. Nanayakkara, M. Challacombe, P.M.W. Gill, B. Johnson, W. Chen, M.W. Wong, C. Gonzalez, J.A. Pople, *Gaussian 03*. Gaussian, Wallingford, CT, 2004.
[22] M. Svensson, S. Humbel, R.D.J. Froese, T. Matsubara, S. Sieber, K. Morokuma, J. Phys. Chem. 100 (1996) 19357–19363.
[23] S. Dapprich, I. Komaromi, K.S. Byun, K. Morokuma, M.J. Frisch, J. Mol. Struct. 461 (1999) 1–21.
[24] F. Maseras, Chem. Commun. 19 (2000) 1821–1827.
[25] A.K. Rappe, C.J. Casewit, K.S. Colwell, W.A. Goddard, W.M. Skiff, J. Am. Chem. Soc. 114 (1992) 10024–10035.
[26] A.D. Becke, J. Chem. Phys. 98 (1993) 1372–1377.
[27] C. Lee, W.T. Yang, R.G. Parr, Phys. Rev. B 37 (1988) 785–789.
[28] V.V. Murashov, J. Leszczynski, J. Mol. Struct. 529 (2000) 1–14.
[29] J.E. Delbene, W.B. Person, K. Szczepaniak, J. Phys. Chem. 99 (1995) 10705–10707.